RADAR EVIDENCE OF SUBGLACIAL LIQUID WATER ON MARS. R. Orosei[1], S. E. Lauro[2], E. Pettinelli[2], A. Cicchetti[3], M. Coradini[4], B. Cosciotti[2], F. Di Paolo[1], E. Flamini[5], E. Mattei[2], M. Pajola[6], F. Soldovieri[7], M. Cartacci[3], F. Cassenti[8], A. Frigeri[3], S. Giuppi[3], R. Martufi[8], A. Masdea[9], G. Mitri[5], C. Nenna[10], R. Noschese[3], M. Restano[11] and R. Seu[8], [1]Istituto Nazionale di Astrofisica, Istituto di Radioastronomia, Via Piero Gobetti 81, 30107 Bologna, Italy, [2]Università degli Studi Roma Tre, Dipartimento di Matematica e Fisica, Via della Vasca Navale 63, 00116 Roma, Italy, [3]Istituto Nazionale di Astrofisica, Istituto di Astrofisica e Planetologia Spaziali, Via del Fosso del Cavaliere 80, 00113 Roma, Italy, [4]Agenzia Spaziale Italiana, Via del Politecnico, 00113 Roma, Italy, [5]International Research School of Planetary Sciences, Università degli Studi "Gabriele d'Annunzio", Viale Pindaro 32, 64105 Pescara (PE), Italy, [6]Istituto Nazionale di Astrofisica, Osservatorio Astronomico di Padova, Vicolo Osservatorio 4, 34102 Padova, Italy, [7]Consiglio Nazionale delle Ricerche, Istituto per il Rilevamento Elettromagnetico dell'Ambiente, Via Diocleziano 326, 60103 Napoli, Italy, [8]Università degli Studi di Roma "La Sapienza", Dipartimento di Ingegneria dell'Informazione, Elettronica e Telecomunicazioni, Via Eudossiana 16, 00163 Roma, Italy, [9]E.P. Elettronica Progetti s.r.l., Via Traspontina 24, 00030 Ariccia (RM), Italy, [10]Danfoss Italia, Via Roma 2, 37011 Postal (BZ), Italy, [11]Serco, c/o ESA Centre for Earth Observation, Largo Galileo Galilei 1, 00033 Frascati (RM), Italy.

Introduction: The presence of liquid water at the base of the Martian polar caps was first hypothesized over thirty years ago and has been inconclusively debated ever since. Radio Echo Sounding (RES) is a suitable technique to resolve this dispute, because low frequency radars have been extensively used and successfully employed to detect liquid water at the bottom of terrestrial polar ice sheets. An interface between ice and water, or alternatively between ice and water-saturated sediments, produces bright radar reflections [1]. The Mars Advanced Radar for Subsurface and Ionosphere Sounding (MARSIS) on the Mars Express spacecraft [2] has been developed to perform RES experiments at Mars.

Data properties: Between 29 May 2012 and 27 December 2015, MARSIS surveyed a 200 km-wide area of Planum Australe, centered at 193° E, 81° S (Fig. 1). This area does not exhibit any peculiar characteristics, it is topographically flat and composed of water ice with 10-20% admixed dust [3]. A total of 29 radar profiles were acquired using onboard unprocessed data mode by transmitting closely spaced radio pulses centered at either 3 and 4 MHz, or at 4 and 5 MHz. In most of the investigated area the basal reflection is weak and diffuse, but in some locations it is very sharp and has a greater intensity than the surrounding areas and the surface.

Assuming an average signal velocity of 170 m/μs within the South Polar Layered Deposits (SPLD), close to that of water ice, this bright basal reflector is located about 1.5 km below the surface. The large size of the MARSIS footprint and the diffuse nature of basal echoes outside the bright reflector prevent a detailed reconstruction of the basal topography, but a regional slope from west to east could be discerned. The subsurface area where the bright reflections are concentrated is topographically flat and surrounded by higher ground, except on its eastern side where there is a depression.

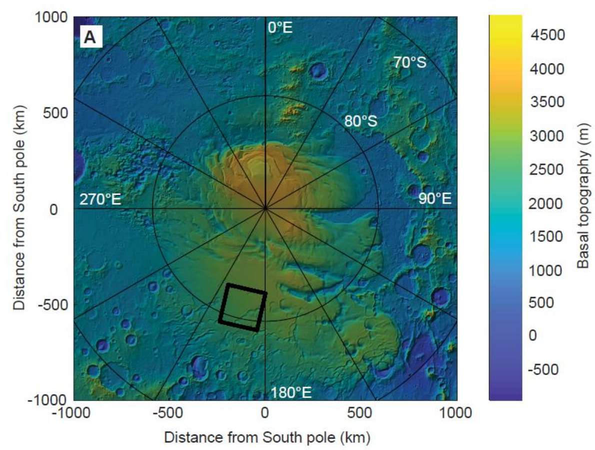

Figure 1: Shaded relief map of Planum Australe, Mars, south of 75°S latitude. The map was produced using the MOLA topographic dataset. The black square outlines the study area.

Analysis: The composition of the material at the base of the SPLD can be inferred from its permittivity, which can be retrieved from the power of the reflected signal. However, the radiated power of the MARSIS antenna is unknown because it could not be calibrated on the ground (due to the instrument's large dimensions), and thus the intensity of the reflected echoes can only be considered in terms of relative quantities. We thus normalized the subsurface echo power to the median of the surface power computed along each orbit, which also compensates any ionospheric attenuation of the signal. Figure 2 shows a regional map of basal echo power after normalization; bright reflections are localized around 193°E, 81°S in all intersecting orbits, outlining a well-defined, 20 km wide subsurface anomaly.

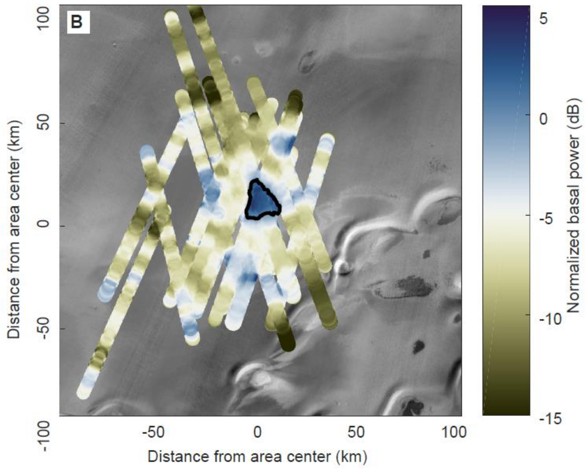

Figure 2: Color-coded map of normalized basal echo power at 4MHz. The large blue area outlined in black corresponds to the main bright area, however the map also shows other small bright spots that have a limited number of overlapping profiles. Background image is a mosaic produced using infrared observations by the THEMIS camera.

To compute the basal permittivity, we also require information about the dielectric properties of the SPLD, which depend on composition and temperature. Because these parameters are only weakly constrained, we run electromagnetic simulations of a plane wave impinging normally onto a three-layer structure representing free space, the SPLD, and the material beneath the SPLD with varying permittivity values. The output of this computation is a family of curves relating the normalized basal echo power to the permittivity of the basal material, which is used to determine the distribution of basal permittivity at the bottom of the SPLD. By determining each possible value of the permittivity corresponding to a measured value of reflectivity, we obtained two distinct distributions of basal permittivity estimates inside and outside the bright reflection area (Fig. 3): median values (at 3, 4 and 5 MHz) are 30±3, 33±1 and 22±1 within the bright area and 9.9±0.5, 7.5±0.1, 6.7±0.1 outside of it.

Interpretation and discussion: The basal permittivity outside the bright area is in the range 4-15, typical for dry terrestrial volcanic rocks. It is also in agreement with previous estimates of 7.5-8.5 for the material at the base of the SPLD [4] and with values derived from radar surface echo power for dense dry igneous rocks on the Martian surface at mid-latitudes [5]. Conversely, permittivity values as high as those found within the bright area have not previously been observed on Mars. RES data collected both in Antarctica [6] and in Greenland [7] show that a permittivity larger than 15 is indicative of the presence of liquid water below the polar deposits. Based on the evident analogy of the physical phenomena on Earth and Mars, we can infer that the high permittivity values retrieved for the bright area below the SPLD are due to water-saturated materials and/or layers of liquid water.

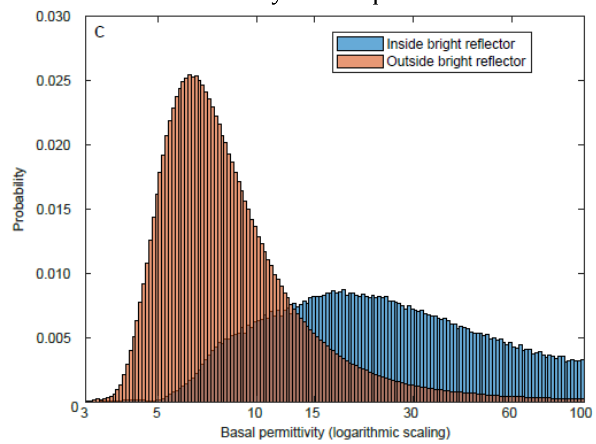

Figure 3: Basal permittivity distributions inside (blue) and outside (brown) the bright reflection area. The non-linear relationship between the normalized basal echo power and the permittivity produces an asymmetry (skewness) in the distributions of the values.

Perchlorates can form through different mechanisms [8] and were detected in different areas of Mars. Because the temperature at the base of the polar deposits is estimated to be around 205 K [9] and because perchlorates strongly suppress the freezing point of water (to a minimum of 198 K for calcium perchlorate) [10], liquid water could be present as a layer of perchlorate brine. The limited raw data coverage of the SPLD (a few percent of the area of Planum Australe) and the large size required for a meltwater patch to be detectable by MARSIS (several kilometers in diameter, several tens of centimeters in thickness) limit the possibility to identify small bodies of liquid water or the existence of any hydraulic connection between them. Because of this, there is no reason to conclude that the presence of subsurface water on Mars is limited to a single location.

References: [1] Carter S. P. et al. (2007) *Geochem. Geophys., 8,* Q03016. [2] Picardi G. et al. (2005) *Science, 310*, 1925-1928. [3] Li J. et al. (2012) *JGR Planets*, 117, E04006. [4] Zhang Z. et al. (2008) *JGR Planets*, 113, E05004. [5] Mouginot J. et al. (2010) *Icarus, 210,* 612-625. [6] Peters M. E. et al. (2005) *JGR Solid Earth,* 110, B06303. [7] Oswald G. K. A. and Gogineni S. P. (2008) *J. Glaciol., 54,* 94-106. [8] Catling D. C. et al. (2010) *JGR Planets 115,* E00E11. [9] Fisher D. A. et al. (2010) *JGR Planets 115,* E00E12. [10] Hecht M. H. et al. (2009) *Science, 325*, 64-67.